

# Quasi-two-dimensional Fermi surfaces of the heavy-fermion superconductor $\text{Ce}_2\text{PdIn}_8$

K. Götze,<sup>1</sup> J. Klotz,<sup>1</sup> D. Gnida,<sup>2</sup> H. Harima,<sup>3</sup> D. Aoki,<sup>4,5</sup> A. Demuer,<sup>6</sup>  
S. Elgazzar,<sup>7</sup> J. Wosnitza,<sup>1</sup> D. Kaczorowski,<sup>2</sup> and I. Sheikin<sup>6,\*</sup>

<sup>1</sup>*Hochfeld-Magnetlabor Dresden (HLD-EMFL), Helmholtz-Zentrum  
Dresden-Rossendorf and TU Dresden, D-01314 Dresden, Germany*

<sup>2</sup>*Institute of Low Temperature and Structure Research,  
Polish Academy of Sciences, P.O. Box 1410, PL-50-950 Wrocław, Poland*

<sup>3</sup>*Graduate School of Science, Kobe University, Kobe 657-8501, Japan*

<sup>4</sup>*IMR, Tohoku University, Oarai, Ibaraki 311-1313, Japan*

<sup>5</sup>*INAC/SPSMS, CEA Grenoble, 38054 Grenoble, France*

<sup>6</sup>*Laboratoire National des Champs Magnétiques Intenses (LNCMI-EMFL), CNRS, UJF, 38042 Grenoble, France*

<sup>7</sup>*Highly Correlated Matter Research Group, Department of Physics,  
University of Johannesburg, P.O. Box 524, Auckland Park 2006, South Africa*

(Dated: September 10, 2015)

We report low-temperature de Haas-van Alphen (dHvA) effect measurements in magnetic fields up to 35 T of the heavy-fermion superconductor  $\text{Ce}_2\text{PdIn}_8$ . The comparison of the experimental results with band-structure calculations implies that the  $4f$  electrons are itinerant rather than localized. The cyclotron masses estimated at high field are only moderately enhanced, 8 and 14  $m_0$ , but are substantially larger than the corresponding band masses. The observed angular dependence of the dHvA frequencies suggests quasi-two-dimensional Fermi surfaces in agreement with band-structure calculations. However, the deviation from ideal two dimensionality is larger than in  $\text{CeCoIn}_5$ , with which  $\text{Ce}_2\text{PdIn}_8$  bears a lot of similarities. This subtle distinction accounts for the different superconducting critical temperatures of the two compounds.

PACS numbers: 71.18.+y, 71.27.+a, 74.70.Tx

The appearance of unconventional superconductivity in the vicinity of a quantum critical point (QCP) is a common trend in Ce-based heavy-fermion (HF) compounds. A more recent and still somewhat controversial issue is the influence of the Fermi-surface (FS) dimensionality on unconventional superconductivity. Indeed, reduced dimensionality of the FS leads to nesting-type magnetic instabilities [1] and thus enhances the superconductivity [2, 3]. The exact knowledge of the FS topology of HF systems is, therefore, essential. In addition, this information allows distinguishing if the  $f$  electrons are itinerant or localized, i.e. whether they contribute to the FS or not.

$\text{Ce}_2\text{PdIn}_8$  is a recently discovered HF superconductor with  $T_c = 0.7$  K and a non-magnetic ground state [4, 5]. Non-Fermi-liquid behavior was observed in both macroscopic [6–10] and microscopic [11, 12] measurements at low temperature, implying that  $\text{Ce}_2\text{PdIn}_8$  is located very close to a QCP. It was further suggested that a two-dimensional (2D) SDW-type QCP is induced by magnetic field near the upper critical field,  $H_{c2} \approx 2$  T [9]. Unconventional superconductivity was demonstrated to be due to antiferromagnetic quantum fluctuations [13]. These unusual properties are strikingly similar to those of the well-studied HF superconductor  $\text{CeCoIn}_5$  [14–17], which is also located very close to a QCP at ambient pressure. However, the superconducting critical temperature  $T_c = 2.3$  K of  $\text{CeCoIn}_5$  [18] is considerably higher than that of  $\text{Ce}_2\text{PdIn}_8$ .

$\text{Ce}_2\text{PdIn}_8$  crystallizes into a tetragonal  $\text{Ho}_2\text{CoGa}_8$ -

type crystal structure with space group  $P4/mmm$ . It belongs to the larger family of  $\text{Ce}_n\text{TIn}_{3n+2}$  ( $T$ : transition metal,  $n = 1, 2$ , and  $\infty$ ) systems, containing a sequence of  $n$   $\text{CeIn}_3$  layers intercalated by a  $\text{TIn}_2$  layer along the  $c$  axis. While cubic  $\text{CeIn}_3$  ( $n = \infty$ ) is a completely isotropic system, the layered structures with  $n = 1$  and 2 are expected to lead to anisotropic properties and quasi-2D FSs. Indeed, quasi-2D FS sheets were observed in both  $n = 1$  systems  $\text{CeCoIn}_5$  [19, 20],  $\text{CeIrIn}_5$  [21],  $\text{CeRhIn}_5$  [22, 23] and the  $n = 2$  compound  $\text{Ce}_2\text{RhIn}_8$  [24, 25]. The degree of two dimensionality is expected to be larger in monolayer systems with alternating layers of  $\text{CeIn}_3$  and  $\text{TIn}_2$  than in their bilayer counterparts, in which two  $\text{CeIn}_3$  layers are separated by one  $\text{TIn}_2$  layer.

In this paper, we report high-field dHvA measurements of  $\text{Ce}_2\text{PdIn}_8$ . The observed FS is quasi-2D, however, we find that the more three-dimensional crystal structure of  $\text{Ce}_2\text{PdIn}_8$  relative to  $\text{CeCoIn}_5$  leads to a reduced two dimensionality of the FS topology. We argue that this can explain the difference in the superconducting critical temperatures of the two compounds.

Single crystals were grown by the self-flux method [4], and we have confirmed by specific-heat measurements that they are not contaminated by  $\text{CeIn}_3$ . The dHvA measurements were performed using a torque cantilever magnetometer mounted in a top-loading dilution refrigerator equipped with a low-temperature rotator. Magnetic fields,  $B$ , up to 35 T generated by LNCMI-Grenoble resistive magnets were applied at different angles between

the [001] and [100] directions.

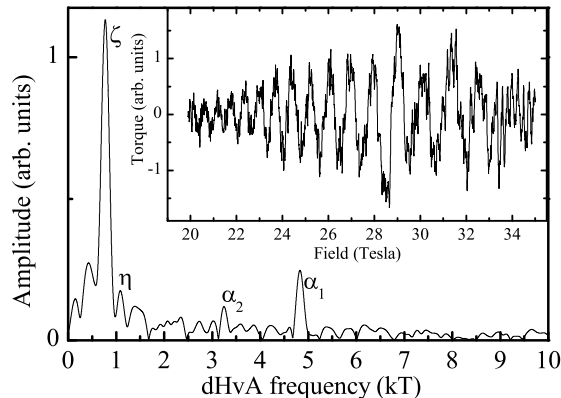


FIG. 1. Fourier spectrum of the high-field dHvA oscillations (inset) in  $\text{Ce}_2\text{PdIn}_8$  for magnetic field applied at  $4^\circ$  off the  $c$  axis at 30 mK.

Figure 1 shows the oscillatory torque after subtracting a non-oscillating background and the corresponding Fourier transform in  $\text{Ce}_2\text{PdIn}_8$ . Four fundamental frequencies, denoted  $\zeta$ ,  $\eta$ ,  $\alpha_1$ , and  $\alpha_2$ , are observed when  $B$  is applied close to the  $c$  axis. The oscillations were traced up to  $60^\circ$ , where their amplitude decreased below the noise level.

To figure out whether the  $f$  electrons are itinerant or localized in  $\text{Ce}_2\text{PdIn}_8$ , we performed band-structure calculations for both  $\text{Ce}_2\text{PdIn}_8$  and  $\text{La}_2\text{PdIn}_8$ , the latter corresponding to the Ce compound with localized  $f$  electrons. For both compounds, the calculations were carried out using a full potential augmented plane wave method with the local density approximation (LDA) for the exchange-correlation potential. As crystals of  $\text{La}_2\text{PdIn}_8$  are currently unavailable, the lattice parameters of  $\text{Ce}_2\text{PdIn}_8$  were used for the  $\text{La}_2\text{PdIn}_8$  calculations. The resulting FSs are shown in Fig. 2.

Given the layered crystal structure, it is not surprising that some of the calculated FS sheets are quasi-2D in both  $\text{Ce}_2\text{PdIn}_8$  and  $\text{La}_2\text{PdIn}_8$ . The details of the FSs are, however, clearly different. In contrast, the topology of the  $4f$ -itinerant FS of  $\text{CeCoIn}_5$  is similar to the  $4f$ -localized FS of  $\text{LaRhIn}_5$  and  $\text{CeRhIn}_5$  [22, 23], where the two FSs differ mainly by size. It should be noted that  $\text{CeCoIn}_5$  is a compensated metal with equal carrier numbers of electrons and holes, while  $\text{LaCoIn}_5$  is an uncompensated metal. On the other hand, both  $\text{Ce}_2\text{PdIn}_8$  and  $\text{La}_2\text{PdIn}_8$  are compensated metals. As seen in Fig. 2, the charge-carrier number given by the FS volume in  $\text{Ce}_2\text{PdIn}_8$  is about two times smaller than that in  $\text{La}_2\text{PdIn}_8$ .

Figure 3(a) shows the experimentally observed angular dependence of the dHvA frequencies in  $\text{Ce}_2\text{PdIn}_8$  together with the results of band-structure calculations based on the  $4f$ -itinerant band model. Experimental and calculated frequencies and effective masses are also shown

Branch	Experiment		Calculation	
	$F$ (kT)	$m^*/m_0$ <sup>a</sup>	$F$ (kT)	$m_b/m_0$
$\gamma$	—	—	0.34	1.55
$\delta$	—	—	0.43	0.42
$\zeta$	0.78	$8.4 \pm 0.4$	0.69	1.24
$\eta$	1.2	—	1.07	2.27
$\alpha_2$	3.26	—	2.82	0.81
$\alpha_1$	4.82	$14 \pm 1$	4.82	2.12
$\beta_2$	—	—	7.27	2.81
$\beta_1$	—	—	13.08	5.2

<sup>a</sup> The effective masses were measured with magnetic field applied at  $4^\circ$  off the  $c$  axis

TABLE I. Experimental and calculated dHvA frequencies and effective masses in  $\text{Ce}_2\text{PdIn}_8$  for magnetic field along the  $c$  axis.

in Table I. The agreement between the experimentally observed  $\alpha$  branches and those of the calculations is excellent. Not only the angular dependences are the same, but even the absolute values agree very well. This implies that both the topology and the size of the calculated FS sheet reproduce the experimental results exceptionally well. The  $\alpha$  branches correspond to the quasi-2D FS of the band 73, as shown in Fig. 2. Regarding the measured lower ( $< 2$  kT) dHvA frequencies, there is also a very good agreement between the experimental and calculated branches. These branches originate mostly from rather isotropic parts of the FS in band 72. The calculated  $\beta$  branches originating from complicated sheets in band 72 were, however, not observed in the experiment. This is probably caused by a strongly enhanced effective mass or an unfavorable curvature factor for detecting the dHvA signal. For comparison, in Fig. 3(b) we plot the experimental results obtained in  $\text{Ce}_2\text{PdIn}_8$  together with band-structure calculations for  $\text{La}_2\text{PdIn}_8$ . In this case, the two are obviously at odds with each other. In particular, only one quasi-2D FS was observed in the experiment, while the calculations predict two of them for  $\text{La}_2\text{PdIn}_8$ , which should be easy to detect.

The comparison of the experimentally observed dHvA frequencies with the results of the LDA band-structure calculations thus gives clear evidence for a quasi-2D FS with itinerant  $f$  electrons in  $\text{Ce}_2\text{PdIn}_8$ . The same conclusion was drawn for  $\text{CeCoIn}_5$  [19, 20].

We, alternatively, calculated the band structure using the local spin density approximation with the relativistic version of the full-potential local orbital method [26] for  $\text{Ce}_2\text{PdIn}_8$ . This also suggests quasi-2D FS, but the agreement with the experimental results is not as good.

The effective masses shown in Table I were determined by fitting the temperature dependence of the oscillatory amplitude by the standard Lifshitz-Kosevich formula [27]. This was done for the magnetic field applied at  $4^\circ$  off the  $c$  axis. Due to the small amplitudes of the

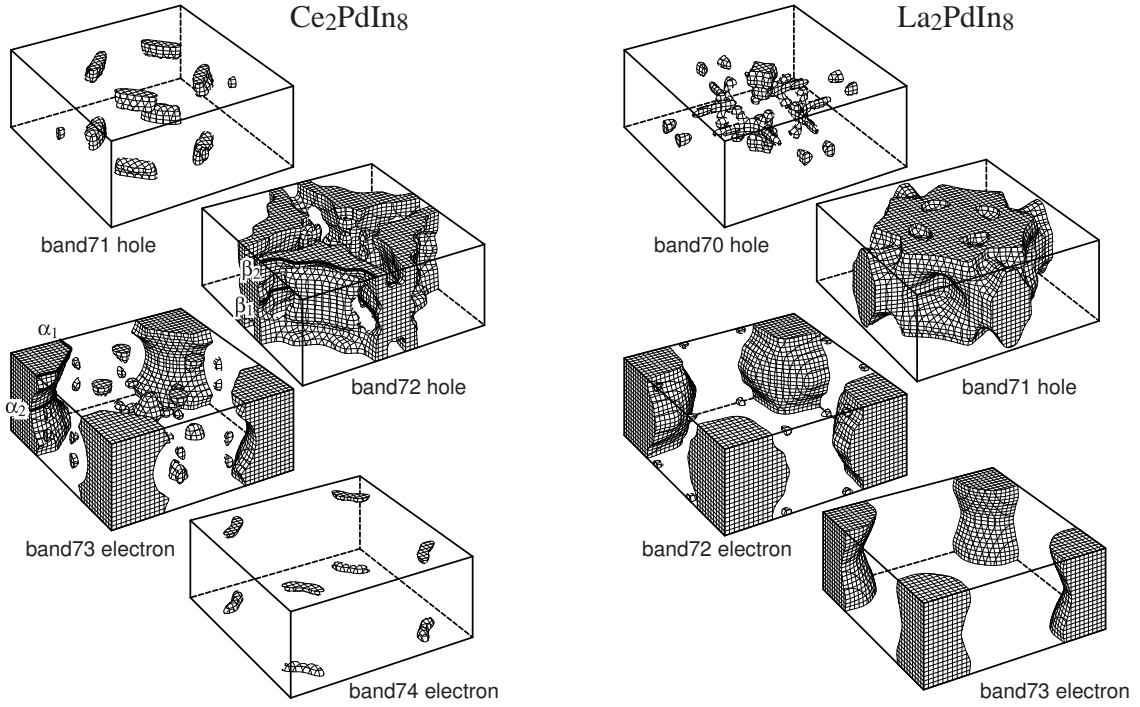


FIG. 2. Calculated FSs of  $\text{Ce}_2\text{PdIn}_8$  (left). Calculated FSs of  $\text{La}_2\text{PdIn}_8$  (right) are also shown for comparison.

oscillations the field range from 28 to 34.5 T was used for the analysis. Even for such high fields, the effective masses of only two branches,  $\zeta$  and  $\alpha_1$ , could be reliably determined. The obtained values are  $8.4 \pm 0.4$  and  $14 \pm 1$   $m_0$ , respectively. The effective mass of the  $\alpha_1$  branch corresponding to the quasi-2D sheet of the FS is comparable to the values, 8 - 18  $m_0$ , reported for the quasi-2D FS of  $\text{CeCoIn}_5$  [19, 20, 28]. This implies a similar degree of hybridization between the  $f$  and conduction electrons. The detected effective masses are, however, by far too small to account for the huge value of the electronic specific heat coefficient,  $\gamma$ , of the order of 1 J/K<sup>2</sup>mol just above the superconducting transition [4, 5, 9]. Presumably, the effective masses of the  $\beta$  branches, which are not observed here, are strongly enhanced. Indeed, already the calculated band masses of the  $\beta$  branches are higher than those of the other branches (see Table I). On the other hand, the Sommerfeld coefficient of  $\text{Ce}_2\text{PdIn}_8$  is similar to that of  $\text{CeCoIn}_5$  [18], where the effective masses were reported to strongly decrease with magnetic field [19]. While the observed dHvA oscillations in  $\text{Ce}_2\text{PdIn}_8$  are not strong enough to perform the field-dependent analysis of the effective masses, they can also be expected to decrease with magnetic field. This assumption is supported by the experimentally observed field dependence of the  $T^2$ -coefficient in the resistivity [6] and of the Sommerfeld coefficient of the specific heat [9] above the upper critical field.

As shown in Fig. 4, the major FS sheets of both  $\text{Ce}_2\text{PdIn}_8$  and  $\text{CeCoIn}_5$  are quasi-2D corrugated cylin-

ders extending along the [001] direction. As many of the physical properties of HF materials strongly depend on the FS dimensionality, the key question here is which FS is more 2D, i.e. which amplitude of the corrugation is smaller. For both  $\text{Ce}_2\text{PdIn}_8$  and  $\text{CeCoIn}_5$ , the FSs experimentally determined through dHvA measurements are in excellent agreement with calculated ones. This is, however, not always the case. That is why we introduce a quantitative criterion of a quasi-2D FS deviation from an ideal cylinder:  $\Delta = (S_{\max} - S_{\min})/\bar{S}$ , where  $S_{\max}$  and  $S_{\min}$  are the maximum and minimum extremal cross-sections respectively, and  $\bar{S}$  is the average cross-section of the warped cylinder. For an ideal cylinder,  $\Delta = 0$ . Since the extremal cross-sections,  $S_i$ , of the FS are proportional to the dHvA frequencies,  $F_i$ ,  $S$  can be replaced by  $F$  measured with field along [001] to determine  $\Delta$  experimentally. In  $\text{Ce}_2\text{PdIn}_8$ , with the two frequencies,  $\alpha_1$  and  $\alpha_2$ , listed in Table I, this yields  $\Delta = 0.386$ . The dHvA effect measurements in  $\text{CeCoIn}_5$  revealed three extremal cross-section of the quasi-2D FS [19, 20, 28]. The reported values of the dHvA frequencies are slightly different, yielding the average value of  $\Delta = 0.221$ . This implies that the deviation from the ideal 2D FS is much smaller in  $\text{CeCoIn}_5$  than in  $\text{Ce}_2\text{PdIn}_8$ . This is expected as well from the more 3D crystal structure of  $\text{Ce}_2\text{PdIn}_8$  as compared to  $\text{CeCoIn}_5$ .

The corresponding larger anisotropy of  $\text{CeCoIn}_5$  as compared to  $\text{Ce}_2\text{PdIn}_8$  accounts for the higher superconducting critical temperature of  $\text{CeCoIn}_5$ . In fact, 2.3 K in  $\text{CeCoIn}_5$  is the highest  $T_c$  among all the known Ce-based

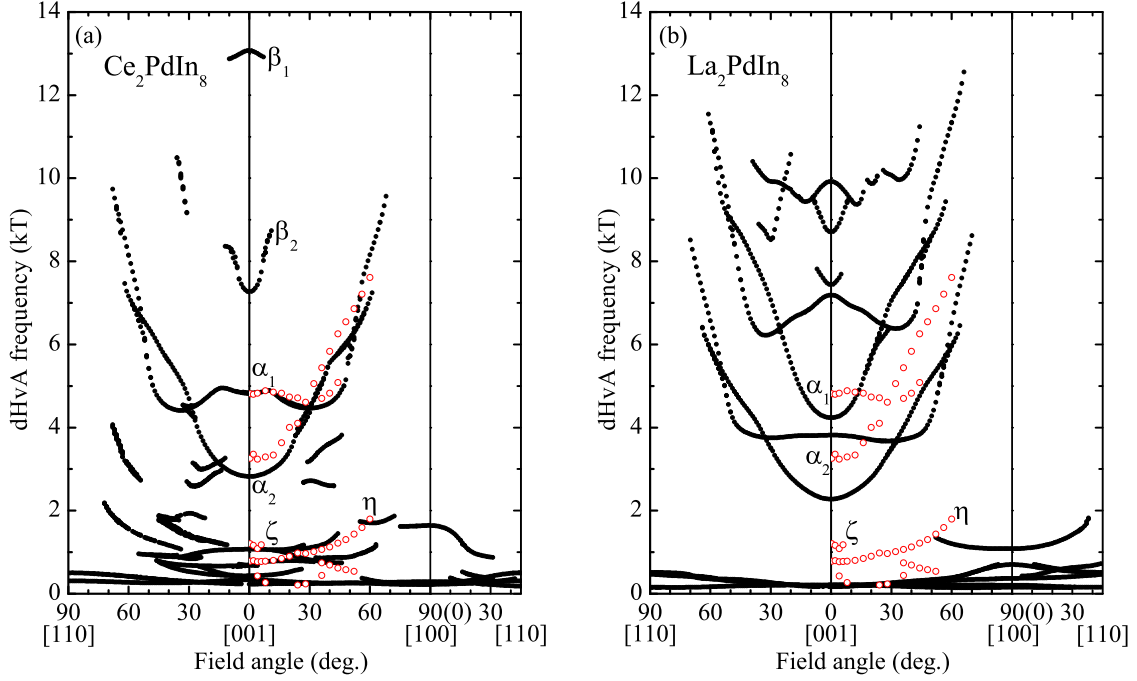


FIG. 3. (color online) Angular dependence of the experimentally observed dHvA frequencies in  $\text{Ce}_2\text{PdIn}_8$  (big open circles) is shown together with the results of band-structure calculations (small closed circles) performed for  $\text{Ce}_2\text{PdIn}_8$  (a) and  $\text{La}_2\text{PdIn}_8$  (b). The latter correspond to  $\text{Ce}_2\text{PdIn}_8$  with localized  $4f$  electrons and are shown for comparison. Very low calculated dHvA frequencies that correspond to small FS pockets are not shown for clarity.

HF materials. Remarkably, the FS of  $\text{CeCoIn}_5$  is the most 2D like as compared to its Ir and Rh analogs [20]. The FS of  $\text{CeRhIn}_5$ , however, changes at its critical pressure  $P_c \simeq 2.4$  GPa [29], and the reported dHvA frequencies yield  $\Delta = 0.17$  above  $P_c$ . This value is similar to that of  $\text{CeCoIn}_5$  at ambient pressure. In  $\text{CeRhIn}_5$ , superconductivity emerges around  $P_c$ , where  $T_c = 2.1$  K [30], a value close to that of  $\text{CeCoIn}_5$ . Regarding  $\text{CeIrIn}_5$ , experimentally observed dHvA frequencies [21] result in  $\Delta = 0.269$ , a value in between those for  $\text{CeCoIn}_5$  and  $\text{Ce}_2\text{PdIn}_8$ . However,  $T_c = 0.4$  K of  $\text{CeIrIn}_5$  [31] can not be compared directly to the critical temperatures of  $\text{CeCoIn}_5$  and  $\text{Ce}_2\text{PdIn}_8$ , as  $\text{CeIrIn}_5$  is located further away from a QCP [32]. When  $\text{CeIrIn}_5$  is tuned to a QCP by Rh substitution,  $T_c$  increases to about 1 K [33], and is likely to be reduced due to disorder as compared to pure compounds. Consistently with  $\Delta$ , this value also falls in between those for  $\text{CeCoIn}_5$  and  $\text{Ce}_2\text{PdIn}_8$ . Unfortunately, there is currently no information about the FS of Rh-substituted  $\text{CeIrIn}_5$ . While the FS dimensionality is not the only factor that determines  $T_c$  in HF superconductors, it is certainly a significant one. Indeed,  $T_c = 18.5$  K was reported for  $\text{PuCoGa}_5$  [34], which is the highest among those yet observed in  $f$ -electron materials. Remarkably, the calculated FS of  $\text{PuCoGa}_5$  consists of three corrugated cylinders [35], although the degree of corrugation is relatively high with  $\Delta$  being 0.448, 0.359 and 0.66 respectively. However, the results of these cal-

culations are still to be confirmed experimentally.

In summary, our high-field dHvA investigation of  $\text{Ce}_2\text{PdIn}_8$  combined with band-structure calculations evidence the existence of a quasi-2D FS with itinerant  $f$ -electrons in this compound. The comparison of the FS topology of  $\text{Ce}_2\text{PdIn}_8$  and  $\text{CeCoIn}_5$  implies that the FS of the latter compound is much closer to an ideal cylinder characteristic for a 2D case. The difference in the FS dimensionality accounts for different superconducting critical temperatures of the two compounds, which are both located in close vicinity to a QCP and have a similar degree of hybridization between the  $4f$  and conduction electrons. It would be interesting to apply the quantitative criterion of the FS two dimensionality we introduced here to other HF materials with quasi-2D FS. In particular, the criterion can be used to verify the theoretical prediction about the influence of the FS dimensionality on the type of quantum criticality in HF compounds [36–39]. Another interesting question is whether magnetic fields themselves affect the FS dimensionality in  $\text{Ce}_2\text{PdIn}_8$  in particular and other quasi-2D HF materials in general. Zero-field ARPES measurements in  $\text{Ce}_2\text{PdIn}_8$  would be very useful to address this issue.

We are grateful to T. Maehira for sharing with us the details of the band-structure calculations in  $\text{PuCoGa}_5$ . KG acknowledges support from the DFG within GRK 1621. We acknowledge the support of the HLD-HZDR and the LNCMI-CNRS, members of the European Mag-

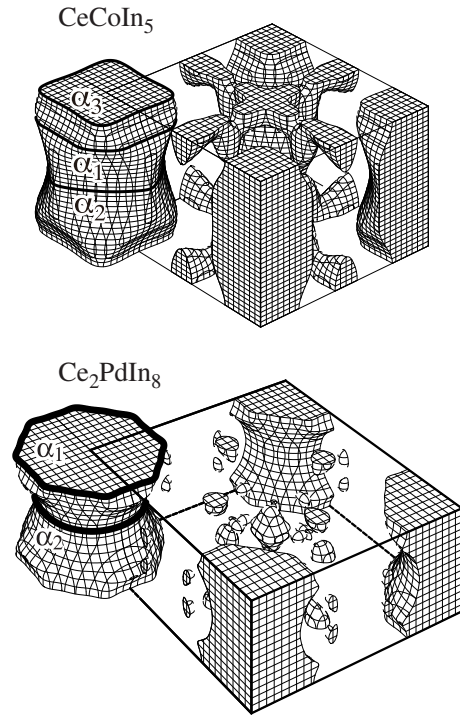


FIG. 4. Comparison of the calculated quasi-2D FSs of  $\text{CeCoIn}_5$  and  $\text{Ce}_2\text{PdIn}_8$ .

netic Field Laboratory (EMFL).

\* ilya.sheikin@lncmi.cnrs.fr

- [1] T. Moriya, Y. Takahashi, and K. Ueda, *J. Phys. Soc. Jpn.* **59**, 2905 (1990).
- [2] P. Monthoux and G. G. Lonzarich, *Phys. Rev. B* **59**, 14598 (1999).
- [3] P. Monthoux, *J. Phys.: Condens. Matter* **15**, S1973 (2003).
- [4] D. Kaczorowski, A. P. Pikul, D. Gnida, and V. H. Tran, *Phys. Rev. Lett.* **103**, 027003 (2009).
- [5] D. Kaczorowski, D. Gnida, A. Pikul, and V. Tran, *Solid State Commun.* **150**, 411 (2010).
- [6] J. K. Dong, H. Zhang, X. Qiu, B. Y. Pan, Y. F. Dai, T. Y. Guan, S. Y. Zhou, D. Gnida, D. Kaczorowski, and S. Y. Li, *Phys. Rev. X* **1**, 011010 (2011).
- [7] V. H. Tran, D. Kaczorowski, R. T. Khan, and E. Bauer, *Phys. Rev. B* **83**, 064504 (2011).
- [8] D. Gnida, M. Matusiak, and D. Kaczorowski, *Phys. Rev. B* **85**, 060508 (2012).
- [9] Y. Tokiwa, P. Gegenwart, D. Gnida, and D. Kaczorowski, *Phys. Rev. B* **84**, 140507 (2011).
- [10] M. Matusiak, D. Gnida, and D. Kaczorowski, *Phys. Rev. B* **84**, 115110 (2011).
- [11] H. Fukazawa, R. Nagashima, S. Shimatani, Y. Kohori, and D. Kaczorowski, *Phys. Rev. B* **86**, 094508 (2012).
- [12] V. H. Tran, A. D. Hillier, D. T. Adroja, and D. Kaczorowski, *Phys. Rev. B* **86**, 094525 (2012).
- [13] K. Hashimoto, Y. Mizukami, R. Katsumata, H. Shishido, M. Yamashita, H. Ikeda, Y. Matsuda, J. A. Schlueter, J. D. Fletcher, A. Carrington, D. Gnida, D. Kaczorowski, and T. Shibauchi, *Proc. Natl. Acad. Sci. U.S.A.* **110**, 3293 (2013).
- [14] J. Paglione, M. A. Tanatar, D. G. Hawthorn, E. Boaknin, R. W. Hill, F. Ronning, M. Sutherland, L. Taillefer, C. Petrovic, and P. C. Canfield, *Phys. Rev. Lett.* **91**, 246405 (2003).
- [15] A. Bianchi, R. Movshovich, I. Vekhter, P. G. Pagliuso, and J. L. Sarrao, *Phys. Rev. Lett.* **91**, 257001 (2003).
- [16] E. D. Bauer, C. Capan, F. Ronning, R. Movshovich, J. D. Thompson, and J. L. Sarrao, *Phys. Rev. Lett.* **94**, 047001 (2005).
- [17] F. Ronning, C. Capan, E. D. Bauer, J. D. Thompson, J. L. Sarrao, and R. Movshovich, *Phys. Rev. B* **73**, 064519 (2006).
- [18] C. Petrovic, P. G. Pagliuso, M. F. Hundley, R. Movshovich, J. L. Sarrao, J. D. Thompson, Z. Fisk, and P. Monthoux, *J. Phys.: Condens. Matter* **13**, L337 (2001).
- [19] R. Settai, H. Shishido, S. Ikeda, Y. Murakawa, M. Nakashima, D. Aoki, Y. Haga, H. Harima, and Y. Onuki, *J. Phys.: Condens. Matter* **13**, L627 (2001).
- [20] D. Hall, E. C. Palm, T. P. Murphy, S. W. Tozer, Z. Fisk, U. Alver, R. G. Goodrich, J. L. Sarrao, P. G. Pagliuso, and T. Ebihara, *Phys. Rev. B* **64**, 212508 (2001).
- [21] Y. Haga, Y. Inada, H. Harima, K. Oikawa, M. Murakawa, H. Nakawaki, Y. Tokiwa, D. Aoki, H. Shishido, S. Ikeda, N. Watanabe, and Y. Onuki, *Phys. Rev. B* **63**, 060503 (2001).
- [22] H. Shishido, R. Settai, D. Aoki, S. Ikeda, H. Nakawaki, N. Nakamura, T. Iizuka, Y. Inada, K. Sugiyama, T. Takeuchi, K. Kindo, T. Kobayashi, Y. Haga, H. Harima, Y. Aoki, T. Namiki, H. Sato, and Y. Onuki, *J. Phys. Soc. Jpn.* **71**, 162 (2002).
- [23] D. Hall, T. P. Murphy, E. C. Palm, S. W. Tozer, Z. Fisk, N. Harrison, R. G. Goodrich, U. Alver, and J. L. Sarrao, *Int. J. Mod. Phys. B* **16**, 3004 (2002).
- [24] T. Ueda, H. Shishido, S. Hashimoto, T. Okubo, M. Yamada, Y. Inada, R. Settai, H. Harima, A. Galatanu, E. Yamamoto, N. Nakamura, K. Sugiyama, T. Takeuchi, K. Kindo, T. Namiki, Y. Aoki, H. Sato, and Y. Onuki, *J. Phys. Soc. Jpn.* **73**, 649 (2004).
- [25] R. Jiang, D. Mou, C. Liu, X. Zhao, Y. Yao, H. Ryu, C. Petrovic, K.-M. Ho, and A. Kaminski, *Phys. Rev. B* **91**, 165101 (2015).
- [26] K. Koepf and H. Eschrig, *Phys. Rev. B* **59**, 1743 (1999).
- [27] D. Shoenberg, *Magnetic oscillations in metals* (Cambridge University Press, 1984).
- [28] A. Polyakov, O. Ignatchik, B. Bergk, K. Götze, A. D. Bianchi, S. Blackburn, B. Prévost, G. Seyfarth, M. Côté, D. Hurt, C. Capan, Z. Fisk, R. G. Goodrich, I. Sheikin, M. Richter, and J. Wosnitzer, *Phys. Rev. B* **85**, 245119 (2012).
- [29] H. Shishido, R. Settai, H. Harima, and Y. Onuki, *J. Phys. Soc. Jpn.* **74**, 1103 (2005).
- [30] H. Hegger, C. Petrovic, E. G. Moshopoulou, M. F. Hundley, J. L. Sarrao, Z. Fisk, and J. D. Thompson, *Phys. Rev. Lett.* **84**, 4986 (2000).
- [31] C. Petrovic, R. Movshovich, M. Jaime, P. G. Pagliuso, M. F. Hundley, J. L. Sarrao, Z. Fisk, and J. D. Thompson, *Europhys. Lett.* **53**, 354 (2001).
- [32] M. Matsumoto, M. J. Han, J. Otsuki, and S. Y. Savrasov, *Phys. Rev. B* **82**, 180515 (2010).
- [33] G.-q. Zheng, N. Yamaguchi, H. Kan, Y. Kitaoka, J. L.

- Sarrao, P. G. Pagliuso, N. O. Moreno, and J. D. Thompson, Phys. Rev. B **70**, 014511 (2004).
- [34] J. L. Sarrao, L. A. Morales, J. D. Thompson, B. L. Scott, G. R. Stewart, F. Wastin, J. Rebizant, P. Boulet, E. Colineau, and G. H. Lander, Nature **420**, 297 (2002).
- [35] T. Maehira, T. Hotta, K. Ueda, and A. Hasegawa, Phys. Rev. Lett. **90**, 207007 (2003).
- [36] Q. Si, J. H. Pixley, E. Nica, S. J. Yammamoto, P. Goswami, R. Yu, and S. Kirchner, J. Phys. Soc. Jpn. **83**, 061005 (2014).
- [37] Q. Si, Physica B **378-380**, 23 (2006).
- [38] Q. Si, Phys. Status Solidi B **247**, 476 (2010).
- [39] J. Custers, K.-A. Lorenzer, M. Müller, A. Prokofiev, A. Sidorenko, H. Winkler, A. M. Strydom, Y. Shimura, T. Sakakibara, R. Yu, Q. Si, and S. Paschen, Nat. Mater. **11**, 189 (2012).